Supporting information for

Handedness-Controlled and Solvent-Driven Actuators with Twisted Fibers

Bo Fang, [a] Youhua Xiao, [a] Zhen Xu, *[a, b] Dan Chang, [a] Bo Wang, [a] Weiwei Gao [a] and Chao Gao [a]*

[a] MOE Key Laboratory of Macromolecular Synthesis and Functionalization, Department of Polymer Science and Engineering, Zhejiang University, 38 Zheda Road, Hangzhou 310027, P. R. China.

[b] National Key Laboratory of Science and Technology on Advanced Composites in Special Environments, Harbin Institute of Technology, Harbin 150080, P. R. China.

*Address correspondence to zhenxu@zju.edu.cn; chaogao@zju.edu.cn

Experimental Section:

Wet-spinning of continuous GO belts. The ready GO suspensions in DMF at a concentration of 10 mg mL^{-1} was loaded into a plastic syringe with a 2-mm-wide micro-fluidic channel, and then being extruded into EA bath at a rate of 20 meters per minute. To guarantee the rapid drying of GO belts, we used organic solvents (DMF & EA) as the dispersive and coagulated agents. The newly formed fibers were drawn out and collected on a scroll and dried for 30 minutes under the heating of infrared lamp in air. The dried fibers were heated in vacuum oven for 2 h at 60 ℃ to remove residual solvents. After the oven cooled down, pure GO belts were obtained.

Fabricating hybrid twisted fibers. GO suspensions in DMF at a concentration of 10 mg mL^{-1} was prepared. To fabricated hybrid fibers, the DMF suspensions of carboxylated multiwall carbon nanotubes (15 mg mL^{-1}) and polyvinyl alcohol (100 mg mL^{-1}) were firstly acquired. Titania nanoparticles with an average diameter size of 100 nm were purchased from *Sinopharm Group Chemical Reagent*. Nanomaterials or polymer and GO suspensions were mixed with a mass faction beyond 50%. All the suspensions were homogeneously mixed by a magnetic stirring apparatus for 2 hours. The mixtures were used as raw materials to be subject to the fabrication of continuous films and twisting-drawing processing. Then we achieved continuous handed hybrid fibers containing nanomaterials or polymer.

Characterization. SEM images were obtained on a Hitachi S4800 field-emission SEM system. POM observations were taken with a Nikon E600POL. The rotary speed of actuators was collected by a UT371 non-contact rotational speed meter, while the

accelerating time was recorded by the captured videos. The generated current of current-alternating device was measured using two-probe method on an electrical transport properties measurement system composing a Keithley 2400 multiple–function source-meter. Mechanical property tests were carried on a HS-3002C at a loading rate of 10% per minute. Confocal laser scanning microscopy observations were conducted on a Zeiss Lsm510 microscopy, using a 488 nm laser to excite with a filtrate around 560 nm.

Rotor kinetic energy. The moment of inertia (J) of a thin copper paddle is calculated as 3×10^{-10} Kg m^{-2} according to the equation ($J=1/12mL^2$), where m and L correspond to the mass (50 mg) and length (8.5 mm) of the cooper paddle, respectively. For the actuation drived by acetone, the average acceleration (α) of the paddle in the initial 0.7 s was calculated as 904 rad/s^2. The mass of the used TGF was ~40 μg. Therefore, the produced initial torsional torque was calculated by $\tau = J\alpha = 2.7 \times 10^{-7}$ N·m. The rotatory speed of the stationary copper paddle was accelerated to a maximum, i.e., ω = 633 rad/s in a short period of 0.7s (t), so the generated peak power output (p) of the rotatory copper paddle is calculated to be 89.3W/kg from the equation ($p = J\omega^2/2t$). The rotor kinetic energy of paddles activated by other solvating species and in Handedness-controlled two units systems is also calculated by the same protocol.

Electrical energy. A magnetic rotor weighing 160 mg was attached at the end of three TGFs system. Five induction coils were connected into an annular and the magnetic rotor was suspended in the circle. When the magnetic rotor was activated by the TGFs, an electrical signal would be produced by an electromagnetic induction principle. A

standard electrochemical workstation CHI660E was connected with induction coils to collect the signal of output voltage (U) and current (I). Using the results of voltage and current, we calculated the value of output electrical power ($P_e = UI$). Since we obtained a triangular waveform for the obtained U/I *vs.* t curve, the output electrical energy (W_e) during the time (Δt) needed for an actuating cycle was calculated by the equation ($W_e = \Delta t P_e/2$). The kinetical-to-electrical energy conversion efficiency was calculated by dividing the peak gravimetric electrical power to the output peak gravimetric rotor mechanical power.

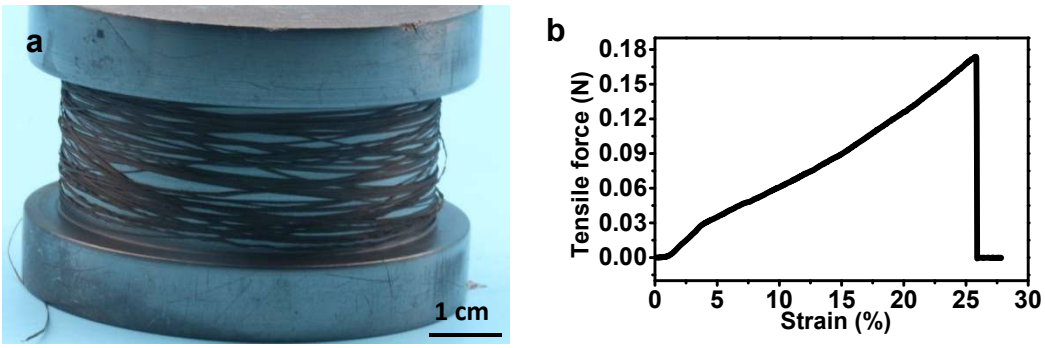

Fig. S1 (a) Continuous GO belts obtained by wet-spinning method. (b) A typical tensile curve of GO belts.

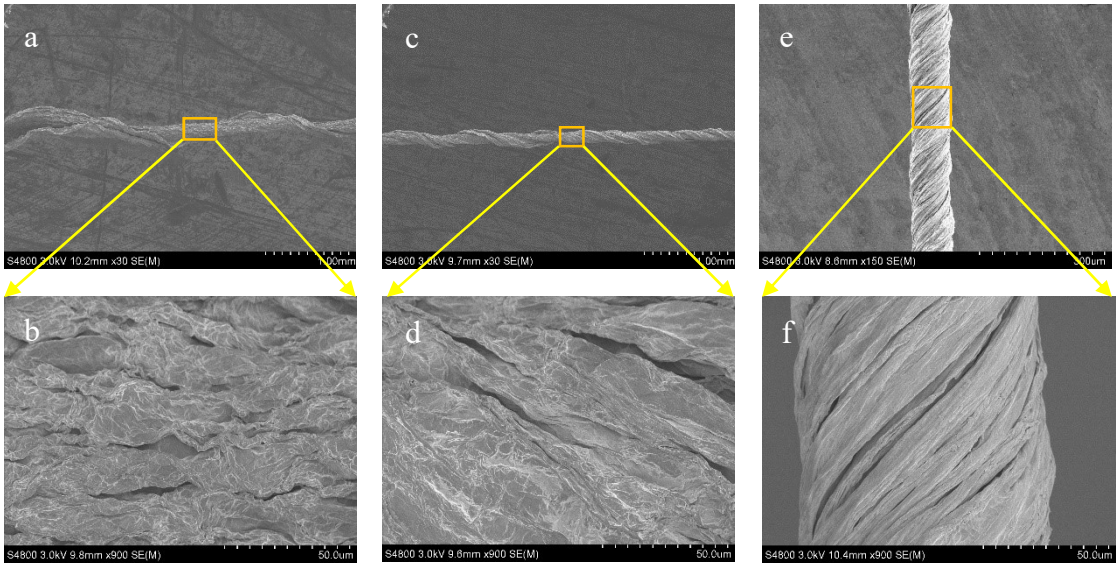

Fig. S2 The evolution of surface structure of GO belts under the twisting collecting process. (a-b) SEM images of GO belt near feeding head, showing an axially orientated structure; (c-d) SEM images of GO belt near orientor, showing the direction of surface wrinkles starts to arrange tipsily; (e-f) SEM images of twisted GO fibers. (g) Continuous GO belts and TGFs.

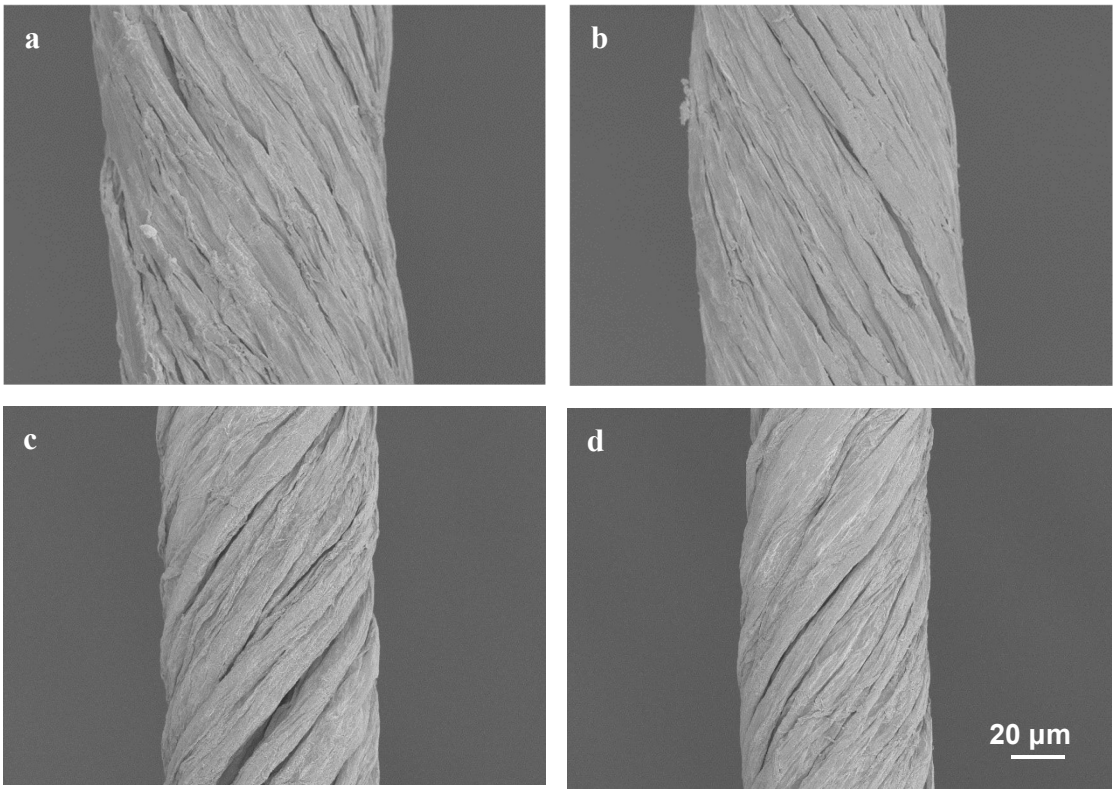

Fig. S3 SEM images of TGFs with the diameter of 118 μm, 97 μm, 83 μm and 68 μm, respectively.

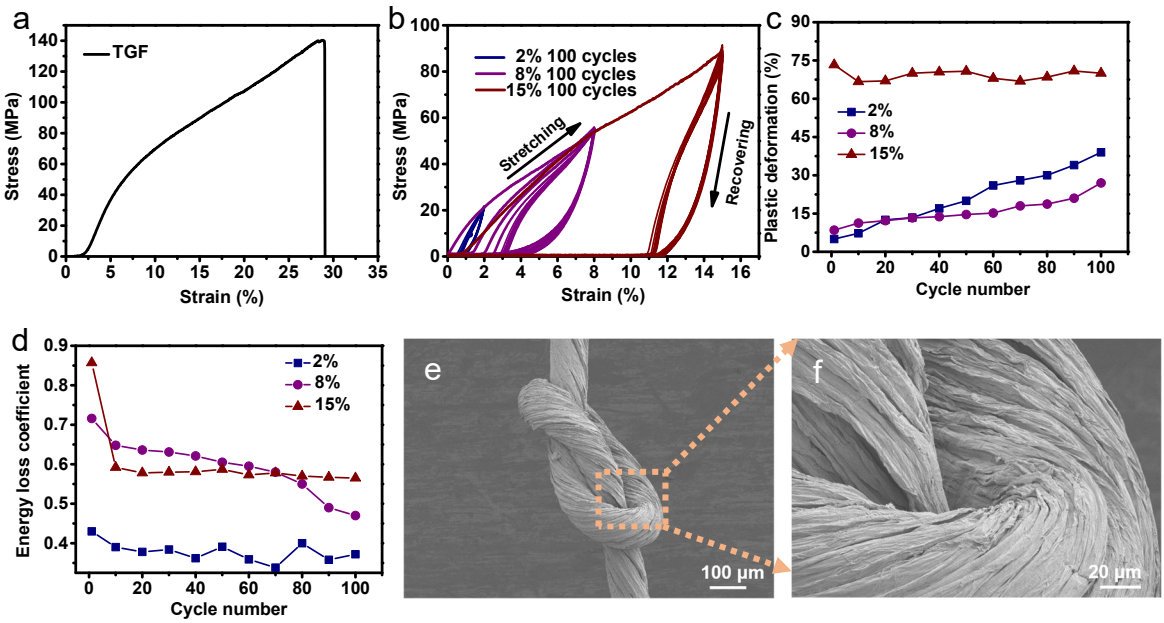

Fig. S4 (a) The measured tensile strength is around 130 MPa, higher than previously reported TGFs obtained from bar-coating films (78 MPa), GO strips (< 10 MPa) and GO gel fibers (110 MPa). In a mechanical durability test at a low elongation of 2% (b), TGF exhibited negligible hysteresis loops after 100 times cycles (c), being ascribed to the reverse stretching of surface wrinkles, as evidenced by the low energy loss coefficient (ELC) of 0.4 (d). When the elongation increases to 8% and 15%, the observable hysteresis loops and the increasing ELC imply a behavior of tensile ductility, being attributed to the irreversibly sheets-to-sheets sliding. However, the unchanged and stable stress (53 MPa at 8%, 88 MPa at 15%) at manifolds cycles confirms the highly reversible stretchability of TGFs. TGF can be tied into tight knots (e), keeping integrating without any crack under the closer observation (f).

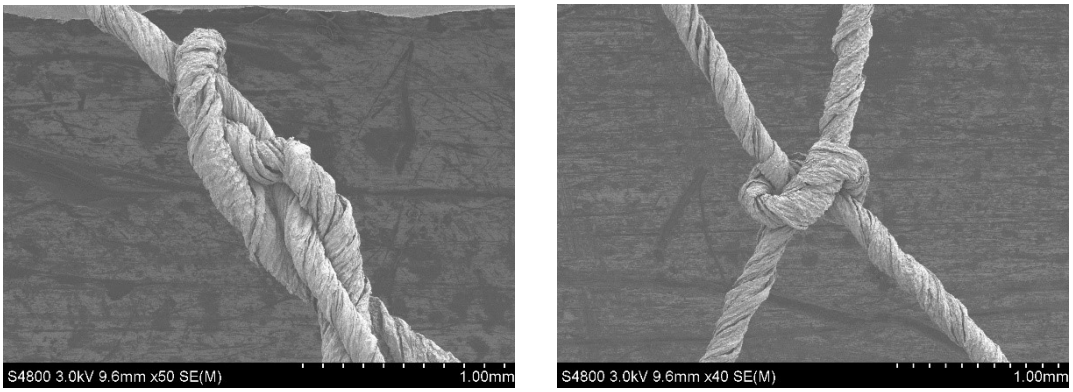

Fig. S5 SEM images of the complex overhand knots tied by continuous TGFs.

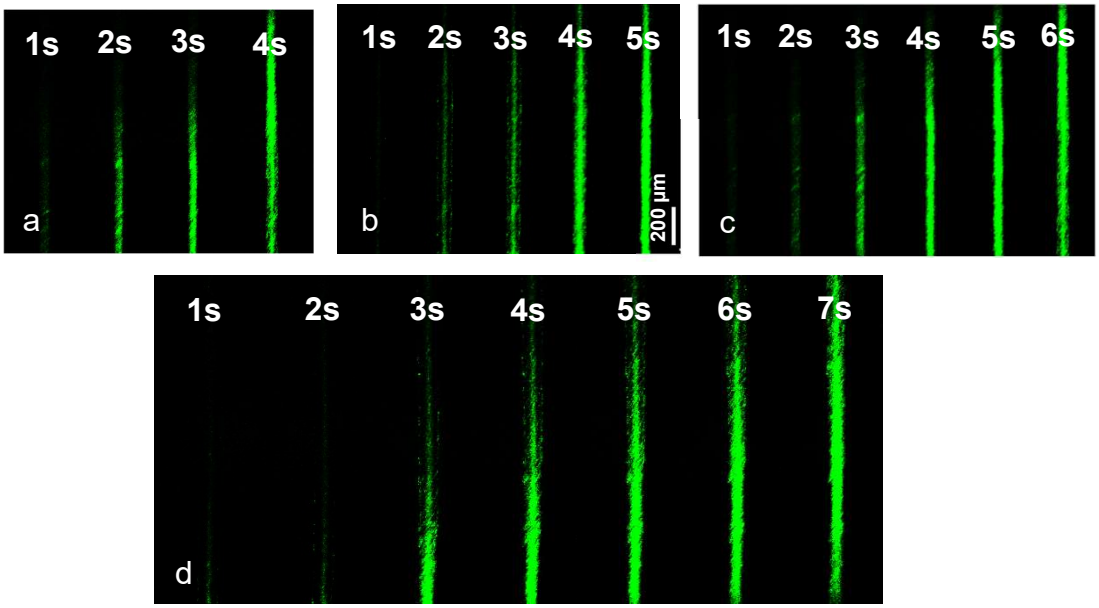

Fig. S6 CLSM observations of the diffusion of acetone(a) ethanol (b), water (c) and methanol (d) on TGF with a constant length of 1.5 mm.

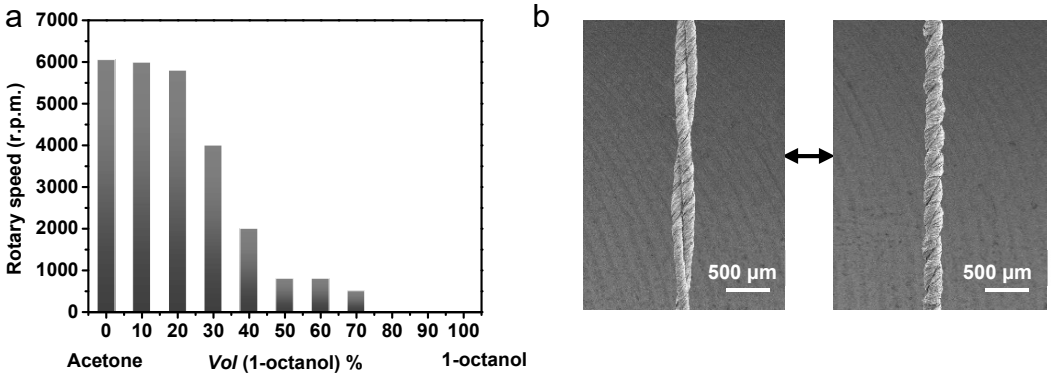

Fig. S7 (a) The relationship of rotary speed of TGFs with the volume ratio of acetone and 1-octanol. (b) SEM images showing the evolution of RR-TGFs system under the successive wetting of acetone.

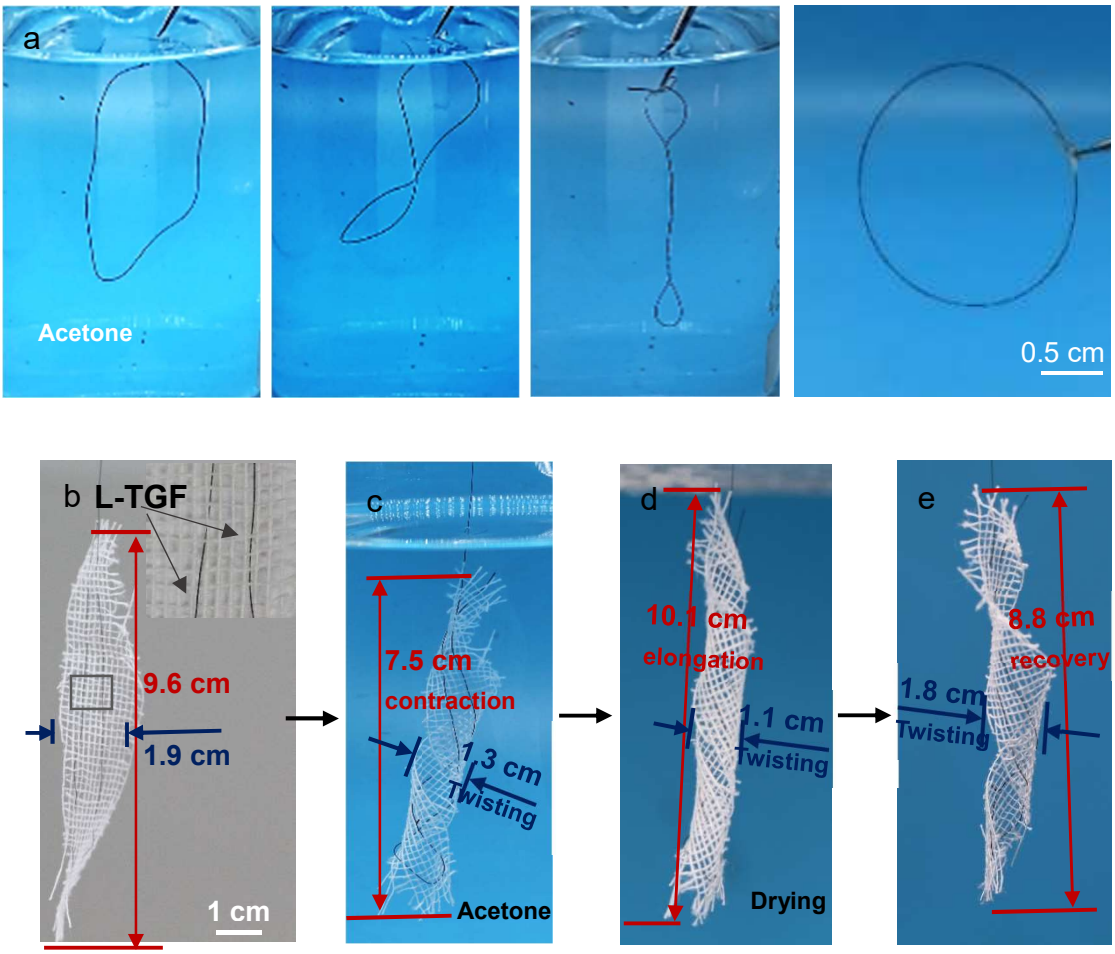

Fig. S8 Ring-like energy harvester has been rarely reported, which can be developed by processing a TGF into a closed circle (a). Provided that this circular fiber is constructed by many individual segments, and all the segments bear synergetic torques from bilateral segments as discussed in RR/LL configuration. Thus, when being wetted by acetone, a torsional deformation occurred and TGF was twisted into a regular coiled form. Solvents removal facilitated the shape recovery. Optical images recording the revolution of ring-like LTGF suffering the soaking of acetone. (b) The monolayer fabric being woven by cotton fibers and a continuous TGF, where the TGF forms a closed pattern. The morphology changes of the fabric when soaking in acetone (c), rotating to the extremity (d) and recover to stretched condition (e) after taking out from acetone bath.

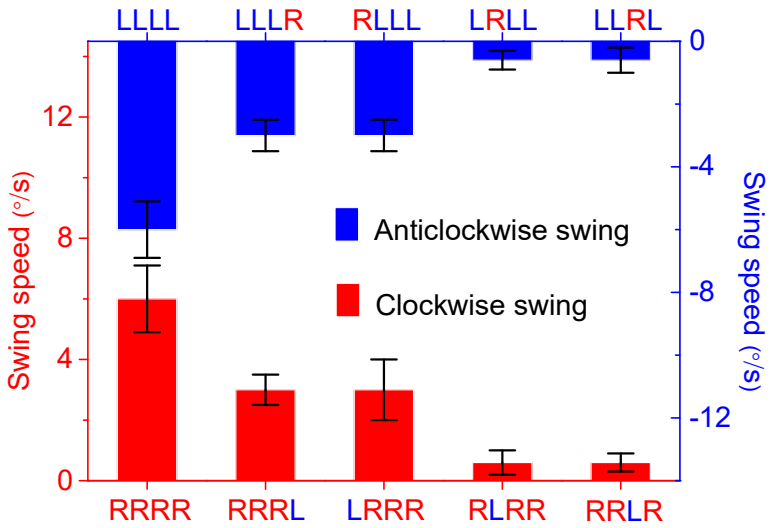

Fig. S9 The relationship of swing direction and speed of four TGFs configurations with the helical chirality arrangement.

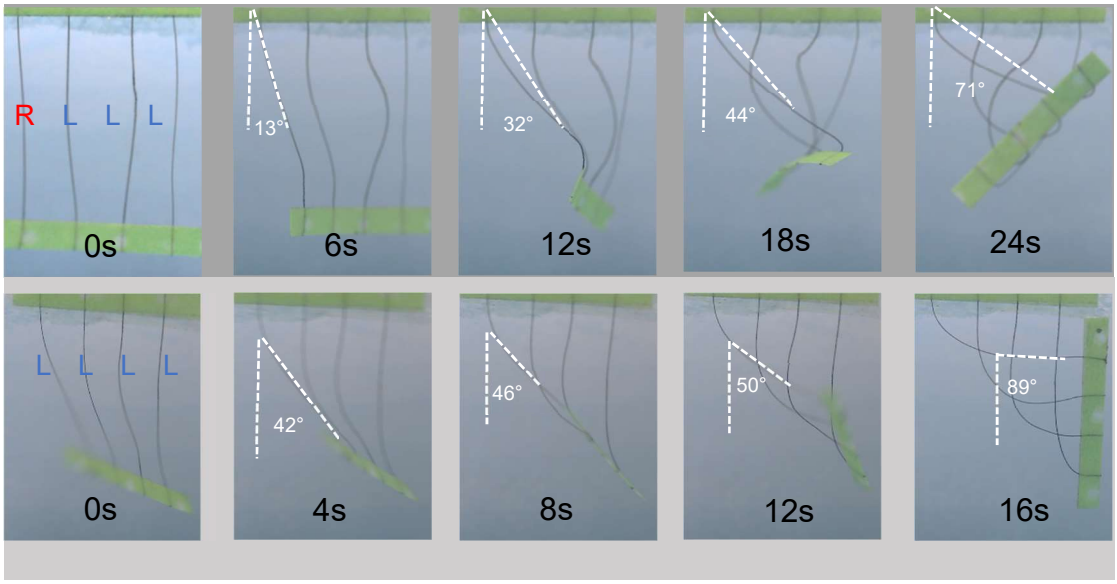

Fig. S10 Programmable gravitational energy harvesters constructed by RLLL and LLLL configurations under the lifting of TGFs, which exhibits the controllable direction and speed of swing.

Table S1. Actuating performance of three-TGFs system with different helical chirality.

	Contracting ratio	Rotary speed of forward	Rotary speed of reverse
RRR-TGFs	3.6%	1764 r.p.m.	544 r.p.m.
LLL-TGFs	3.3%	1620 r.p.m.	590 r.p.m.
RRL-TGFs	2.6%	1149 r.p.m.	394 r.p.m.
RLL-TGFs	2.5%	1256 r.p.m.	319 r.p.m.
RLR-TGFs	1.7%	571 r.p.m.	434 r.p.m.

*Contracting ratio stands for the ratio of lifting height of TGFs to their primary lengths.

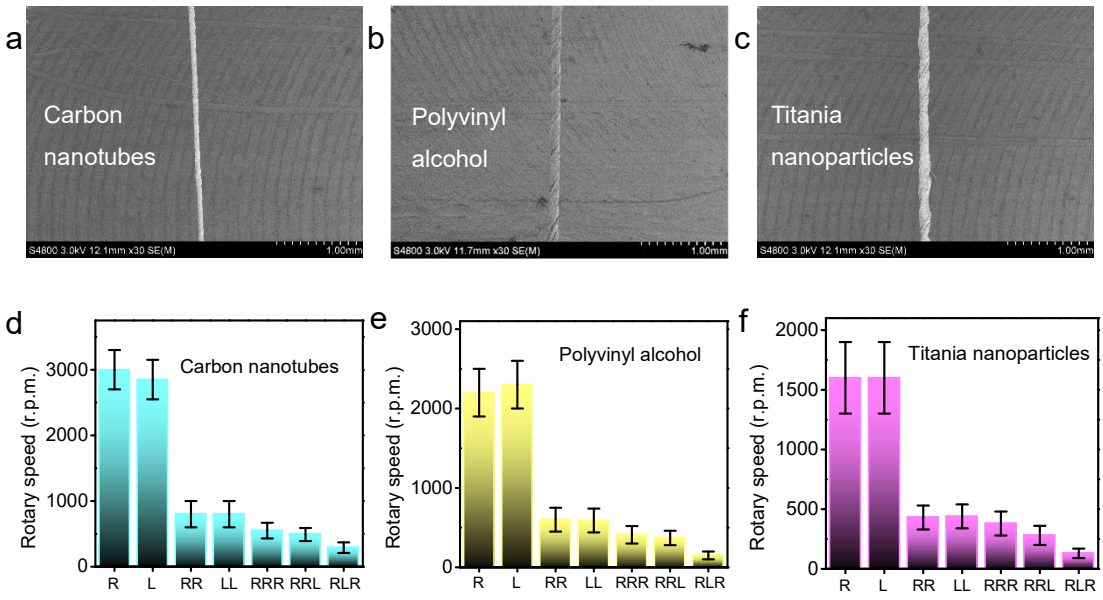

Fig. S11 Continuous hybrid twisted fibers made with graphene oxide and carbon nanotubes (a), polyvinyl alcohol (b), and titania nanoparticles (c). (d-f) The rotary speed of handedness-controlled actuating systems made with hybrid twisted fibers under the driving of 0.05 mL acetone.